Mon. Not. R. Astron. Soc. **000**, 000–000 (0000) Printed 25 April 2014 (MN LATEX style file v2.2)

Analysis of bulk void regions

Sebastian Bustamante ⋆[1] Jaime E. Forero-Romero[2]

[1] *Instituto de Física - FCEN, Universidad de Antioquia, Calle 67 No. 53-108, Medellín, Colombia*
[2] *Departamento de Física, Universidad de los Andes, Cra. 1 No. 18A-10, Edificio Ip, Bogotá, Colombia*

25 April 2014

ABSTRACT

Key words: Cosmology: large-scale Structure of Universe, galaxies: star formation - line: formation

1 INTRODUCTION

The spatial distribution of galaxies describes a web-like pattern, the so-called cosmic web. Today it is understood that such configuration is driven by gravitational instabilities. ...

Relevant information about previous works and current state of the art.

2 THE SIMULATION

As it was previously mentioned, we use an unconstrained cosmological simulation, the Bolshoi simulation, to identify the possible large scale environment of the Local Group. This is a similar approach to the one already used by **[reference here]**.

The Bolshoi simulation follows the non-linear evolution of a dark matter density field on a cubic volume of size $250h^{-1}$Mpc sampled with 2048^3 particles. The cosmological parameters in the simulation are $\Omega_{\rm m} = 0.27$, $\Omega_\Lambda = 0.73$, $h = 0.70$, $n = 0.95$ and $\sigma_8 = 0.82$ for the matter density, cosmological constant, dimensionless Hubble parameter, spectral index of primordial density perturbations and normalization for the power spectrum. The mass of each particle in the simulation is $m_{\rm p} = 1.4 \times 10^8 h^{-1} {\rm M}_\odot$. We identify halos with two algorithms, the Friends-of-Friends **[reference here]** algorithm and the Bound Density Maximum algorithm.

3 ALGORITHMS TO QUANTIFY THE COSMIC WEB

3.1 The tidal web (T-web)

The first algorithm we use to identify the cosmic web is based upon the diagonalization of the tidal tensor, defined as the Hessian of a normalized gravitational potential

$$T_{\alpha\beta} = \frac{\partial^2 \phi}{\partial x_\alpha \partial x_\beta} \tag{1}$$

where the physical gravitational potential has been rescaled by a factor $4\pi G\bar{\rho}$ in such a way that ϕ satisfies the following equation

$$\nabla^2 \phi = \delta, \tag{2}$$

where $\bar{\rho}$ is the average density in the Universe, G is the gravitational constant and δ is the dimensionless matter overdensity.

3.2 The velocity web (V-web)

We also use a kinematical method to define the cosmic-web environment in the simulation. The method has been thoroughly described in XXX and applied to study the shape and spin alignment in the Bolshoi simulation here XX. We refer the reader to these papers to find a detailed description of the algorithm, its limitations and capabilities. Here we summarize the most relevant points for the discussion.

The V-web method for environment finding is based on the local shear tensor calculated from the smoothed DM velocity field in the simulation. The central quantity is the following dimensionless quantity

$$\Sigma_{\alpha\beta} = -\frac{1}{2H_0}\left(\frac{\partial v_\alpha}{\partial x_\beta} + \frac{\partial v_\beta}{\partial x_\alpha}\right) \tag{3}$$

where v_α and x_α represent the α component of the comoving velocity and position, respectively. $\Sigma_{\alpha\beta}$ can be represented by a 3×3 symmetric matrix with real values, that ensures that is possible to diagonalize and obtain three real eigenvalues $\lambda_1 > \lambda_2 > \lambda_3$ whose sum (the trace of $\Sigma_{\alpha\beta}$) is proportional to the divergence of the local velocity field smoothed on the physical scale $\mathcal{R}$.

The relative strength of the three eigenvalues with respect to a threshold value λ_{th} allows for the local classifica-

⋆ sbustama@pegasus.udea.edu.co

tion of the matter distribution into four web types: voids, sheets, filaments and peaks, which correspond to regions with 3, 2, 1 or 0 eigenvalues with values larger than λ_{th}. Below we shall discuss a novel approach to define an adequate threshold value based on the visual impression of void regions, furthermore we study other possible values based on other visual features of the cosmic web.

3.3 The cosmic web in Bolshoi

Both established schemes to quantify the cosmic web depend on continuous and smooth physical quantities, i.e the peculiar velocity field and the density field. To calculate these quantities, a discretization over the volume of the simulation is performed, so all the properties are reduced to single values associated to discrete cells. According to this, we divide the overall volume into $(256)^3$ cells, so each cell has an associated comoving cubic volume of 0.98 Mpc h^{-1}. Finally, in order to reduce possible effects due to the discretization process, a gaussian softening is performed between neighbour cells.

Once defined the numerical details about both classification schemes, we shall analyse the dependence on the threshold value λ_{th} for each one. For this, we shall use the distribution of dark matter halos as tracer of the underlying matter field in order to be more consistent with available observational data. In the figure 1 we calculate fractions of halos within each one of the defined environments based upon the FOF catalogue of the simulation and for an extensive λ_{th} range. Then we look for some key feature that could indicated us a possible optimal value of the λ_{th} value. One first step forward our quest is the behaviour of the V-web scheme compared with the T-web. As was previously established by **Hoffman et al. (2012)** and as can be seen in the figure 1, V-web scheme is significantly more sensible to variations of the λ_{th} value, since all fractions of halos for the V-web change significantly in the range $[0, 0.4]$, whereas, for the T-web scheme, fractions change smoothly throughout all λ_{th} range covered. From this, it is then expected that the optimal λ_{th} value for the V-web scheme is less than the T-web value.

The more notorious characteristic of the figure 1 is the behaviour of the fraction of halos within sheet regions for both web schemes, increasing until a local maximum, and then decreasing. The increasing or decreasing rate of the fraction of halos for some region could be interpreted as a measure of the degree of non-linearity of such region for some specific λ_{th} value. For example, filaments and knots, that are the most non-linear regions of the universe, have a negative rate for all covered λ_{th} range. In the case of voids, the situation is completely opposite, where fractions of halos increase in everywhere. If we think in terms of the underlying matter field of the cosmic web, λ_{th} is just a cutting parameter between high non-linear regions (filament and knots) and low non-linear (voids and sheets). Furthermore, if we take into account that dark matter halos are much more likely to form in high non-linear regions, it is expected the obtained behaviour of fractions of halos for voids, filaments and knots as we increase the λ_{th} value. However, the behaviour of the fraction of halos in sheets is less clear, increasing for low λ_{th} values (like voids) and decreasing for higher λ_{th} values (like filaments and knots). This indicates us the transitional character of sheet regions in the cosmic web. Our proposal here is to select as optimal λ_{th} the value where the fraction of sheets reaches a local maximum, so sheets are completely taken as intermediate transitional and neutral zones regarding the degree of non-linearity. According to this, we find for the T-web scheme an optimal value $\lambda^T_{opt} = 0.36$ and for the V-web scheme $\lambda^V_{opt} = 0.20$. In the figure 2 we show the visual impression of the cosmic web along with the density field for different λ_{th} values including the optimal values. It can be noticed that the optimal values found reproduce well the visual impression.

As we have taken halos as tracers of the cosmic web, we analyse distributions of mass and peculiar velocity in order to assign typical values to each type of environment. In the figure 3 we calculate both distributions for web schemes and using the FOF catalogue of the simulation. Thick lines correspond to the median of the distribution and filled regions limited by dashed lines correspond to quartiles Q_1 and Q_3, it means, 50% of all halos are within such regions for every λ_{th} value and for each type of environment. We rather use median and quartiles as measure of dispersion because there are some very unusual and extreme values that makes the usual analysis based upon means and standard deviations less reliable.

A first interesting feature of the figure 3 is the median mass for each region. In the case of the T-web, although dispersions of the distribution of mass for each environment are considerably overlapped each other, the median value is very well-differentiated among types of environment, indicating that it is possible to assign typical values of mass to each region, and being consistent with expectations, where low mass halos are typical in voids until high mass halos in knots. For the case of the V-web scheme, all medians and dispersions are completely overlapped, specially for values grater than the optimal λ_{th} value, indicating that it is not possible to assign typical mass ranges to each environment as quantified by this scheme. For peculiar velocities, this situation is opposite, where V-web scheme is much more adequate to assign typical distributions of velocity to each environment. Although T-web also makes a differentiation in the distributions of velocity, this is very slight compared with the V-web case. These results can be explained by appealing the physical origin of each web scheme. As T-web is based upon the Hessian matrix of the potential field, it is expected all quantities related to the potential, like density field and distribution of halos mass, are well-differentiated among each region, while for the V-web scheme, based upon the shear velocity tensor, all dynamical quantities, as the peculiar velocity field and the distribution of halos velocity are alike expected to be well-differentiated among regions as quantified by this scheme.

Finally, we also calculate typical distributions of the density and peculiar velocity fields in each type of environment, obtaining completely analogous results. Furthermore, we also use a BDM catalogue of the simulation, obtaining very similar conclusions.

4 FINDING BULK VOIDS

Following the recent growing interest in studying galaxy formation in low-density regions as cosmological tests, we use

a simple method based on a FOF-like algorithm, where we build an input catalogue for the FOF method with the coordinate of the center of every cell marked as void according to the web classification scheme adopted, setting a linking length to connect diagonal neighbour cells. Then, following the work of **Forero-Romero et al. 2008**, we perform a percolation analysis in order to select the best threshold parameter that reduces percolation in cells.

In figure 4 we show the result of our percolation analysis for both web schemes. In both cases, it can be noticed that the volume of the largest void region in the lower panel is minimized at $\lambda_{th} = 0$, what means that percolation is completely reduced for this threshold value. Regarding the number of voids, shown in the upper panel, the T-web scheme presents a expected behaviour, where the number of voids decreases with λ_{th} as the largest void absorbs minor voids through percolation. For the V-web scheme, there is an anomaly around the optimal λ_{th} value, where there is a considerable increment of the number of voids. In the figure 5, we calculate a distribution function of the volume of voids. First for $\lambda_{th} = 0.0$ in the upper panel, where both schemes present similar distributions, although voids in the V-web scheme are slight biased towards middle volume, with a lower abundance for low volume regions than voids in the T-web scheme. Secondly, in the lower panel of this figure, we compute the same distribution of volumes for the optimal parameter previously established for both schemes. Here, it can be noticed a significant over-abundance of low volume voids for the V-web scheme compared with the T-web. As it was above-mentioned from the figure 3, the λ_{th} value can be associated, at least indirectly, to an increase of the threshold value of the peculiar velocity field, in the case of the V-web, or the density field for the T-web. Therefore, the over-abundance of low volume voids for the V-web implies high fluctuations in the peculiar velocity field, while the density field is more robust. In the same plot, it can be noticed a lack of high volume voids, what is also due to percolation, since high volume voids are absorbed by the largest void.

In the light of the previous results, we choose a threshold parameter $\lambda_{th} = 0$ for all subsequent analysis of voids in order to avoid percolation and high fluctuations of the V-web scheme. In spite of this value is quite different to the previously established optimal threshold for each scheme, bulk voids for $\lambda_{th} = 0$ are expected to be the central cores of bulk voids at higher threshold values, assuming that percolation could be reduced. Therefore, global properties of voids are expected to maintain for $\lambda_{th} = 0$.

5 PROPERTIES OF VOIDS

Once defined the proper scheme to classify bulk voids in the simulation, we proceed to analyse their physical properties, like the inertia values, the density and peculiar velocities profiles as calculated over the grid and profiles of number of halos.

5.1 Shape of voids

Quantifying the shape of voids is gaining importance due to cosmological tests such as the Alcock-Paczynski test **[Sutter, et.al (2012)]**, so we compute here the reduced inertia tensor through the next expression in order to determine shape distributions of bulk voids.

$$\tau_{ij} = \sum_{l} \frac{x_{l,i} x_{l,j}}{R_l^2} \tag{4}$$

where l is an index associated to each cell of the current region, i and j indexes run over each spatial direction and finally R_l is defined as $R_l^2 = x_{l,1}^2 + x_{l,2}^2 + x_{l,3}^2$. All positions are measured from the respective geometric center of each void.

The eigenvalues of the reduced inertia tensor, i.e. the principal moments of inertia, are used to quantify the shape of each bulk void. They are denoted as τ_1, τ_2 and τ_3 such that $\tau_1 \leqslant \tau_2 \leqslant \tau_3$. In Figure 6 we show the computed distributions for τ_1/τ_2 and τ_2/τ_3 for voids larger than 8 cells in order to avoid statistic fluctuations due to small regions. We rather calculate histograms for these ratio quantities instead of each single value in order to avoid using an arbitrary normalization. For both schemes, it can be noticed that the shape distribution is completely spread out, thereby indicating a non-preferred geometry of void regions, which is in agreement with the well established high anisotropy of matter flows associated to this type of region.

For a better quantification, we also perform a classification of the shape of voids by setting a threshold in the analysed ratio quantities. An anisotropic or tri-axial shape correspond to voids where $\tau_1/\tau_2 < 0.7$ and $\tau_2/\tau_3 < 0.7$, where there is not any symmetry among the principal directions. We find about $57.2\% \sim 61.0\%$ of total voids consistent with this shape, for the T-web and V-web respectively. A pancake or quasi-oblate shape is associated to voids where $\tau_1/\tau_2 < 0.7$ and $\tau_2/\tau_3 > 0.7$. We found $13.1\% \sim 17.9\%$ of consistent voids. Filamentary or quasi-prolate voids satisfy $\tau_1/\tau_2 > 0.7$ and $\tau_2/\tau_3 < 0.7$, with $25.4\% \sim 18.1\%$ of all voids. Finally, isotropic or quasi-spheric voids are found when $\tau_1/\tau_2 > 0.7$ and $\tau_2/\tau_3 > 0.7$, with $4.2\% \sim 3.1\%$ of total voids compatible with this shape. The threshold value of 0.7 adopted here for the ratios of the moments of inertia is just for illustrative purposes, where such distinction is rather fuzzy and continuous. However, the previous analysis allows us to conclude that voids are quite asymmetric structures.

5.2 Density profile of voids

Describing the density profiles of voids is quite important in order to compare and match simulation with observational surveys, allowing possible constrains for different cosmology models **[Hamaous, et.al 2014]**. Here, and taking into account the previous results, we rather use an ellipsoidal approximation to describe and fit the shape of bulk voids, so we use the next ellipsoidal radial coordinate to describe density profiles.

$$r^2 = \frac{x^2}{\tau_1^2} + \frac{y^2}{\tau_2^2} + \frac{z^2}{\tau_3^2}, \quad 0 \leqslant r \leqslant 1 \tag{5}$$

where we take the principal moments of inertia $\{\tau_i\}$ as the lengths of the principal axes of the ellipsoid and each one of the cartesian coordinates as measured in the rotated frame of each void.

We use the same analytic density profile that **[Hamaous, et.al 2014]** to fit the numerical density profiles of our voids.

$$\delta_v(r) = \delta_c \frac{1-(r/r_s)^\alpha}{1+(r/r_v)^\beta} \tag{6}$$

6 CONCLUSIONS

ACKNOWLEDGMENTS

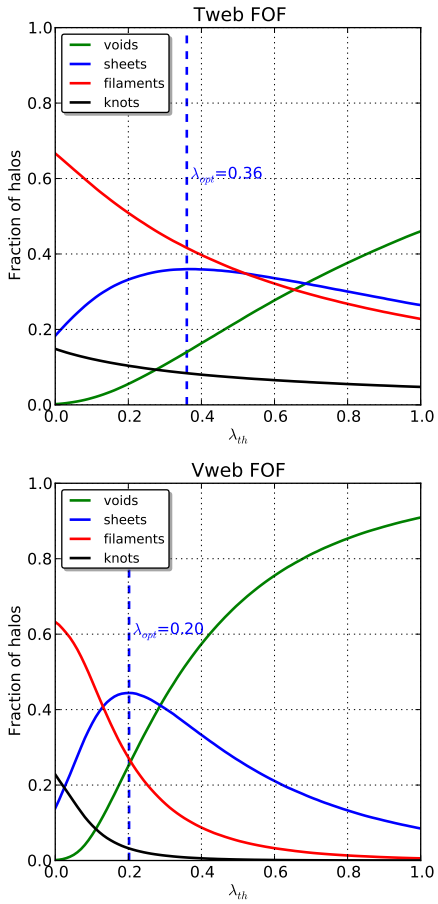

Figure 1. Fractions of halos embedded in each one of the defined environments according to the λ_{th} value. T-web scheme (upper panel) and V-web scheme (lower panel). The optimal parameters found are $\lambda^T_{opt} = 0.36$ and $\lambda^V_{opt} = 0.20$.

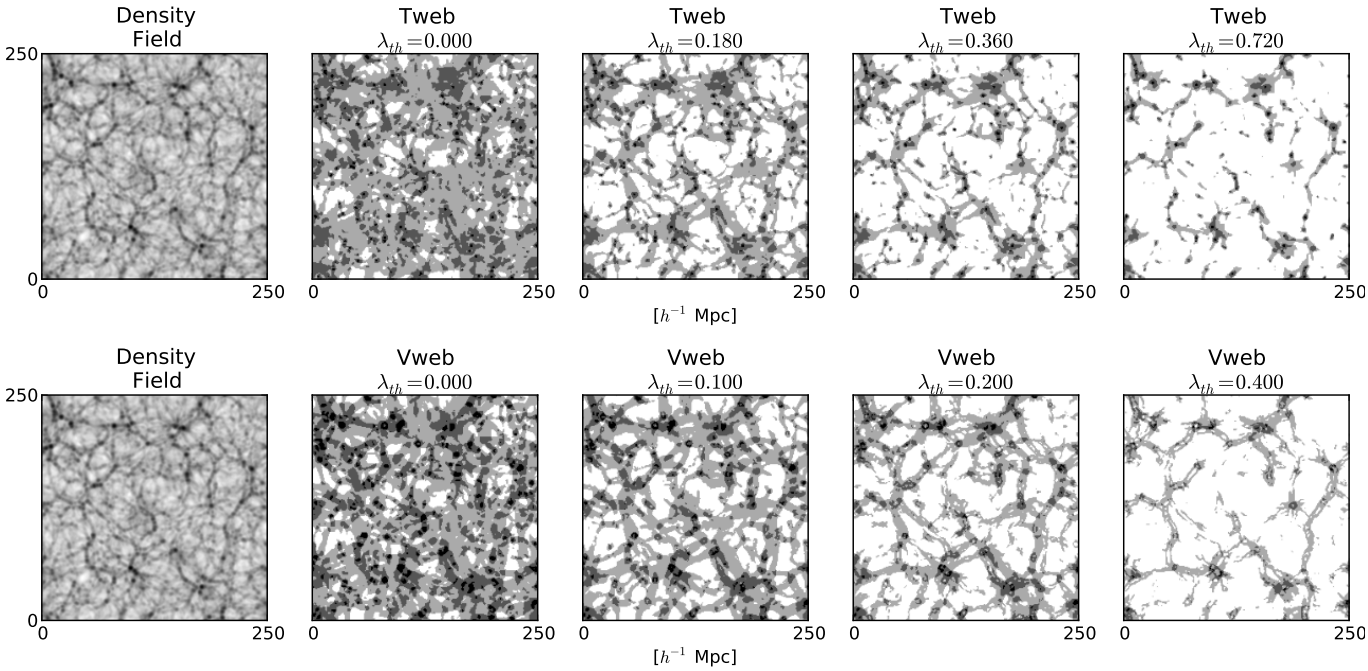

Figure 2. Visual impression of the density field (left panels), and of each classification scheme with the λ_{th} values obtained by our criteria (others panels). The color convention for each environment is (white) - void, (light gray) - sheet, (gray) - filament, (black) - knot. For each web scheme, it has been used the previously established optimal threshold as a reference value, so plots are done with the next values $\lambda_{th} = 0.0$, $\lambda_{th} = \lambda_{opt}/2$, $\lambda_{th} = \lambda_{opt}$ and $\lambda_{th} = 2\lambda_{opt}$.

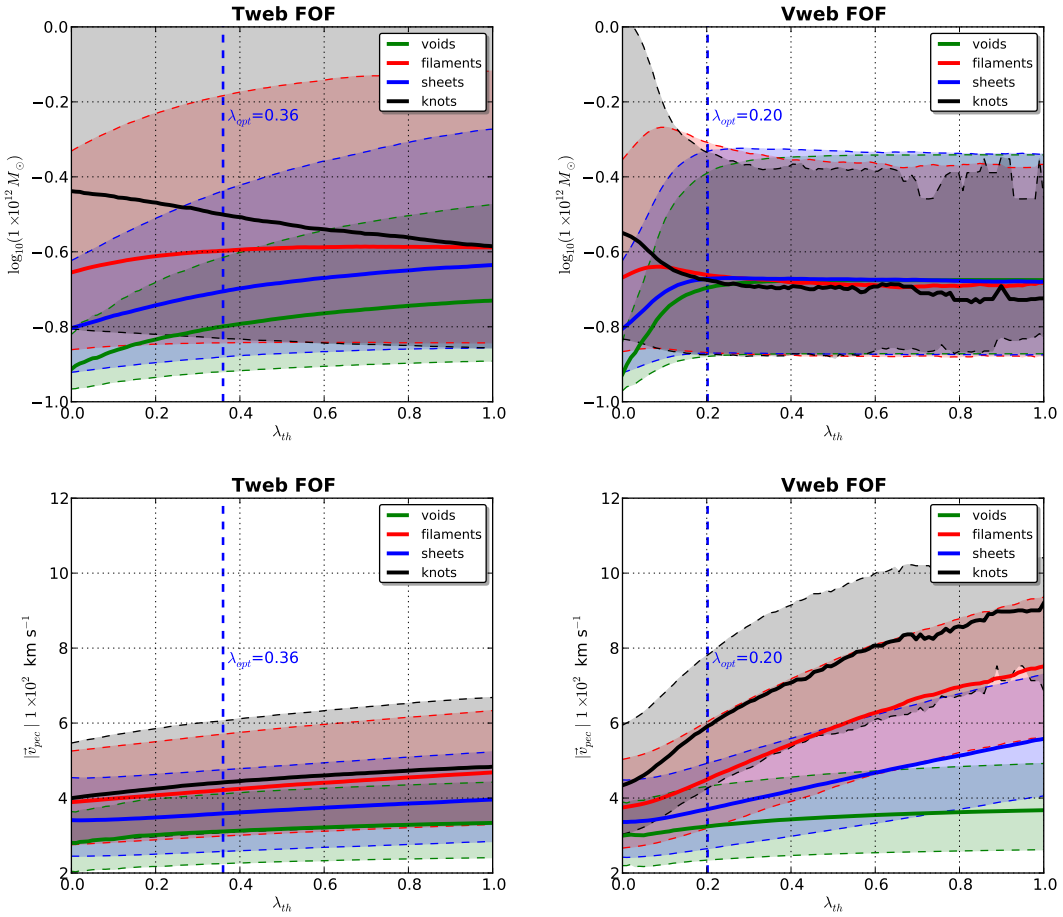

Figure 3. Distribution of masses of dark matter halos according the region where they are embedded for both web schemes (upper panels) and of peculiar velocity (lower panels).

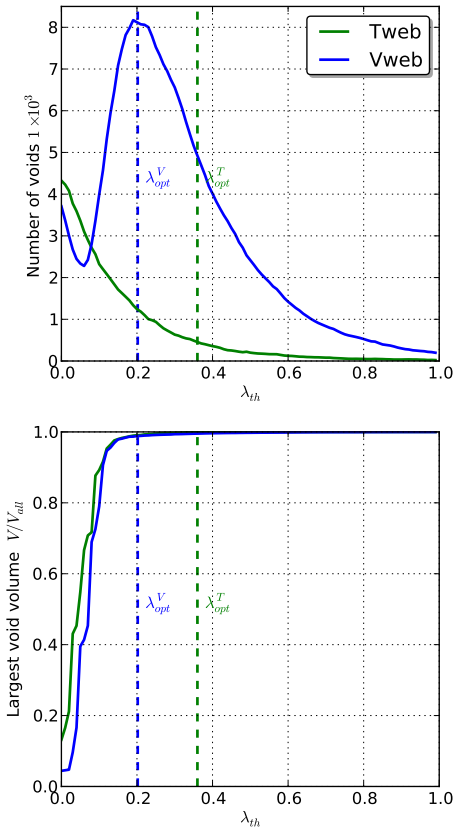

Figure 4. Percolation analysis of bulk void found by using FOF void finder algorithm. It is swept an extensive λ_{th} range for both web schemes. T-web (blue lines) and V-web (green lines). Plot of the largest volume (lower panel) and the number of bulk voids found (upper panel).

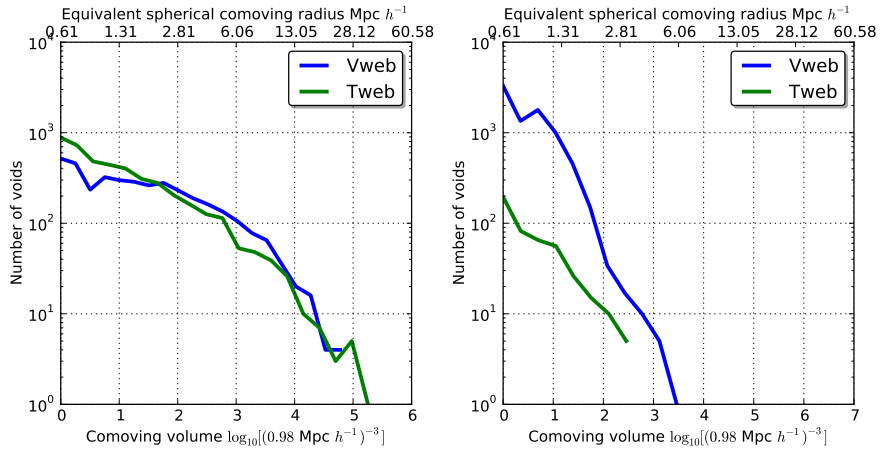

Figure 5. Volume functions of voids for both web schemes. In the upper panel is shown the results for the catalogue generated at $\lambda_{th} = 0.0$, while in the lower panel for the catalogue at $\lambda_{th} = \lambda_{opt}$.

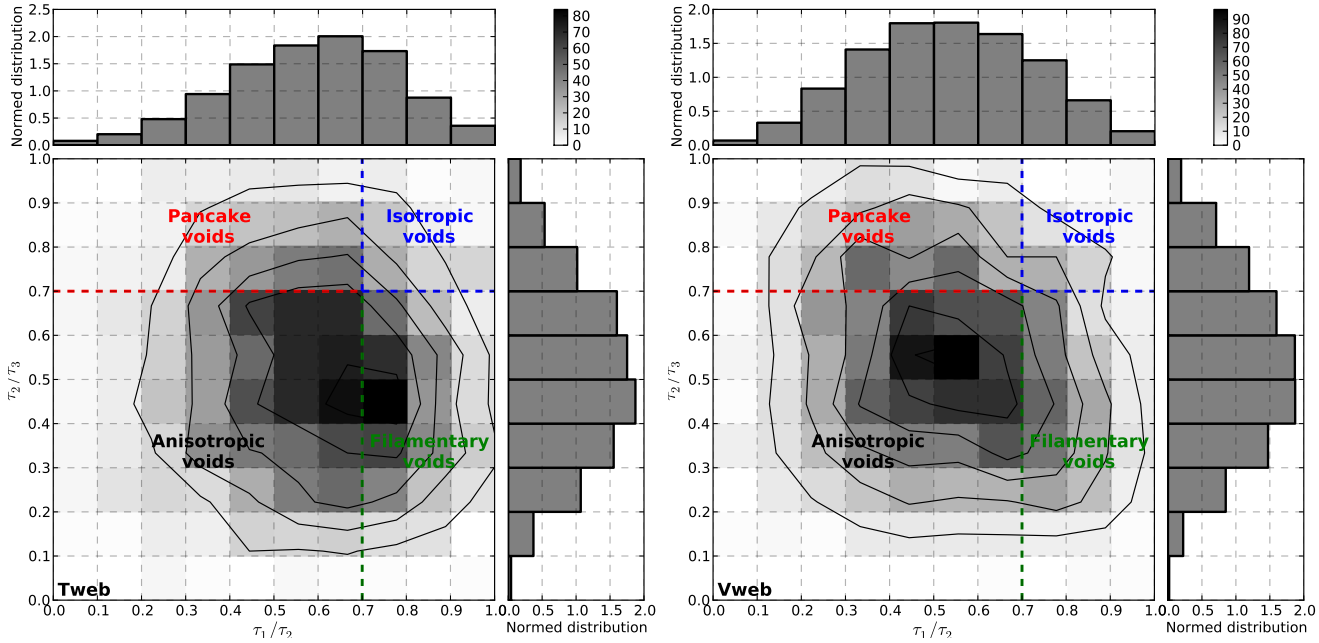

Figure 6. Histogram of eigenvalue ratio τ_1/τ_2 vs τ_2/τ_3 for the inertia tensor of void regions. T-web (upper panel) and V-web (lower panel). Number of cells per region in 2D histograms are indicated by the respective colour bar. Upper (τ_1/τ_2) and right (τ_2/τ_3) panels of each figure shows a normalized histogram of each ratio parameter. The adopted division for quantify the morphology of void regions is not well justified, it should be understood as a fuzzy and continuous limit, done just for illustrative purposes.